Retrograde monosynaptic tracing reveals the temporal evolution of inputs onto new neurons in the adult dentate gyrus and olfactory bulb

Aditi Deshpande^{a,1}, Matteo Bergami^{a,1}, Alexander Ghanem^b, Karl-Klaus Conzelmann^b, Alexandra Lepier^a, Magdalena Götz^{a,c,d}, and Benedikt Berninger^{a,e,f,2}

^aDepartment of Physiological Genomics, Institute of Physiology, Ludwig-Maximilians University Munich, D-80336 Munich, Germany; ^bMax von Pettenkofer Institute and Gene Center, Ludwig-Maximilians-University Munich, D-81377 Munich, Germany; ^cInstitute of Stem Cell Research, Helmholtz Zentrum München, D-85764 Neuherberg, Germany; ^dMunich Cluster for Systems Neurology (SyNergy), 80336 Munich, Germany; ^eInstitute of Physiological Chemistry, and ^fFocus Program Translational Neuroscience of the Johannes Gutenberg University, University Medical Center of the Johannes Gutenberg University, D-55128 Mainz, Germany

Edited by Fred H. Gage, The Salk Institute for Biological Studies, San Diego, CA, and approved February 13, 2013 (received for review November 2, 2012)

Identifying the connectome of adult-generated neurons is essential for understanding how the preexisting circuitry is refined by neurogenesis. Changes in the pattern of connectivity are likely to control the differentiation process of newly generated neurons and exert an important influence on their unique capacity to contribute to information processing. Using a monosynaptic rabies virus-based tracing technique, we studied the evolving presynaptic connectivity of adult-generated neurons in the dentate gyrus (DG) of the hippocampus and olfactory bulb (OB) during the first weeks of their life. In both neurogenic zones, adult-generated neurons first receive local connections from multiple types of GABAergic interneurons before long-range projections become established, such as those originating from cortical areas. Interestingly, despite fundamental similarities in the overall pattern of evolution of presynaptic connectivity, there were notable differences with regard to the development of cortical projections: although DG granule neuron input originating from the entorhinal cortex could be traced starting only from 3 to 5 wk on, newly generated neurons in the OB received input from the anterior olfactory nucleus and piriform cortex already by the second week. This early glutamatergic input onto newly generated interneurons in the OB was matched in time by the equally early innervations of DG granule neurons by glutamatergic mossy cells. The development of connectivity revealed by our study may suggest common principles for incorporating newly generated neurons into a preexisting circuit.

adult neurogenesis | synaptic tracing | adult neural stem cell | functional integration | pseudotransduction

n most mammals, the dentate gyrus (DG) of the hippocampus and the olfactory bulb (OB) are remodeled throughout life by the incorporation of new neurons, with accruing evidence pointing toward unique roles of these neurons in information processing (1-4). Crucial for a better understanding of the contribution of adult-generated neurons to circuit function is the identification of their connectome and how it develops during the process of integration. Optogenetics-based techniques have been successfully used to prove that several weeks following their birth, newborn neurons establish functional contacts with distinct types of postsynaptic partners (5, 6). Along the same vein, previous studies have demonstrated that newborn neurons receive different types of synaptic input at early stages of their functional integration compared with later ones. For example, during the first weeks of life, adult-born DG granule neurons are thought to receive almost exclusively GABAergic input and only later become targets for glutamatergic synapses as well (7). Although synaptogenesis in adult-born neurons has been suggested to follow a distinct pattern of maturation compared with postnatalgenerated neurons, the final connectivity of these two populations of neurons is generally thought to be very similar (8). However, little is known about the precise identity of the synaptic partners at different stages of maturation, both in the DG and OB. Moreover, studying the time line of connectivity of adult-generated neurons is likely to unveil fundamental principles that need to be met for successful incorporation of new neurons into a preexisting neural circuit in the context of brain repair.

Revealing the connectivity of these neurons is a major challenge requiring unbiased techniques for systematically tracing the pre- and postsynaptic partners. A key breakthrough in mapping neuronal connectivity has been the development of a pseudotyped rabies virus (RABV)-based method for monosynaptically restricted tracing of connections between postsynaptic neurons and their first-order presynaptic partners (9). This method is based on targeting primary RABV infection to "starter" cells ectopically expressing TVA, an avian receptor for the envelope protein EnvA used for pseudotyping the RABV (10). Providing these starter cells with the RABV glycoprotein (G) allows for the subsequent retrograde transsynaptic virus transfer to presynaptic partners. By means of single-cell electroporation, adenoassociated virus-mediated transduction or Cre-mediated recombination in transgenic mice, previous strategies have proved the efficient expression of TVA and G in restricted populations of starter cells in vivo (11, 12). The delivery of RABV to and subsequent transfer from these starter cells located in a host of neuroanatomical regions, such as the cerebral cortex and the

Significance

New neurons are constantly added to the hippocampus and the olfactory bulb. These neurons are believed to fulfill unique functions during their early life compared with mature neurons, which may depend on the way they are connected. Here we studied the stepwise integration of new neurons within these two brain areas using a rabies-virus-based synaptic tracing tool. Our study revealed that in both areas integration follows a similar logic, with adult-born neurons incorporating first into the local circuit before becoming innervated by longrange connections. This changing pattern of presynaptic connectivity likely contributes to adult-born neurons' functions.

Author contributions: A.D., M.B., M.G., and B.B. designed research; A.D. and M.B. performed research; A.G., K.-K.C., and A.L. contributed new reagents/analytic tools; A.D., M.B., and B.B. analyzed data; and A.D., M.B., M.G., and B.B. wrote the paper.

The authors declare no conflict of interest.

This article is a PNAS Direct Submission.

¹A.D. and M.B. contributed equally to this work.

²To whom correspondence should be addressed. E-mail: berningb@uni-mainz.de.

This article contains supporting information online at www.pnas.org/lookup/suppl/doi:10. 1073/pnas.1218991110/-/DCSupplemental.

spinal cord, allowed for successfully mapping the connections established by specific sets of short- and long-range presynaptic partners (13, 14). Most recently, two different retrovirus-based approaches were used to restrict primary RABV infection to adult-generated neurons in the DG, disclosing both local and long-range connections (1, 15). However, these studies did not investigate the connectivity at the early phase of integration [i.e., before DG granule neurons receive input from the entorhinal cortex (EC)].

Adult neural stem cells (aNSCs) in the subgranular zone (SGZ) of the DG generate intermediate progenitors that ultimately give rise to glutamatergic granule neurons (16). Similarly, the subependymal zone (SEZ) harbors aNSCs, which give rise to neuroblasts that migrate tangentially along the rostral migratory stream (RMS) to the OB. There, the neuroblasts migrate radially and differentiate into various types of interneurons populating both the granule cell layer (GCL) and the glomerular layer (17, 18). We therefore adapted the RABV-based monosynaptic tracing technique to target adult-generated neurons for primary RABV infection. To this end, we directed the expression of both TVA and G via retroviral vectors selectively to newborn neurons in the DG and the RMS/OB and subsequently transduced these with RABV encoding a reporter gene, to identify their presynaptic connections from early to late stages of maturation. Using this technique we were able to unveil similarities and differences in the evolution of innervations of newly generated neurons in both neurogenic regions, suggesting adherence to a common logic that governs incorporation into preexisting circuits of the adult brain.

Results

RABV-Based Tracing of Local Presynaptic Partners in the DG. To render adult-generated neurons susceptible to primary infection by the EnvA-pseudotyped RABV and capable of retrograde transfer to the immediate presynaptic partners, we designed a polycistronic retroviral vector encoding *G*, *TVA*, and the fluorescence reporter *DsRedExpress2* to visualize transduced cells (Fig. 1*A*). Fig. 1*B* depicts our general strategy for monosynaptic tracing of presynaptic partners of adult-generated neurons in vivo.

Stereotactic delivery of *G* and *TVA*-encoding retrovirus and RABV (Fig. 1*C*) resulted in the appearance of double reporter-positive granule neurons, indicating they had undergone double transduction (Fig. 1*D*). Patch-clamp recording of RABV-infected adult-generated neurons showed no overt differences in their electrical properties compared with those transduced with retrovirus alone (Fig. S1). We also observed neurons expressing GFP only, indicating transsynaptic spread of RABV from the double-transduced newborn granule neurons (Fig. 1*D*). Voluntary exercise is known to increase cell proliferation, survival, and synaptogenesis of newborn neurons in the DG (19, 20). Although we observed an increase in retroviral transduction efficiency

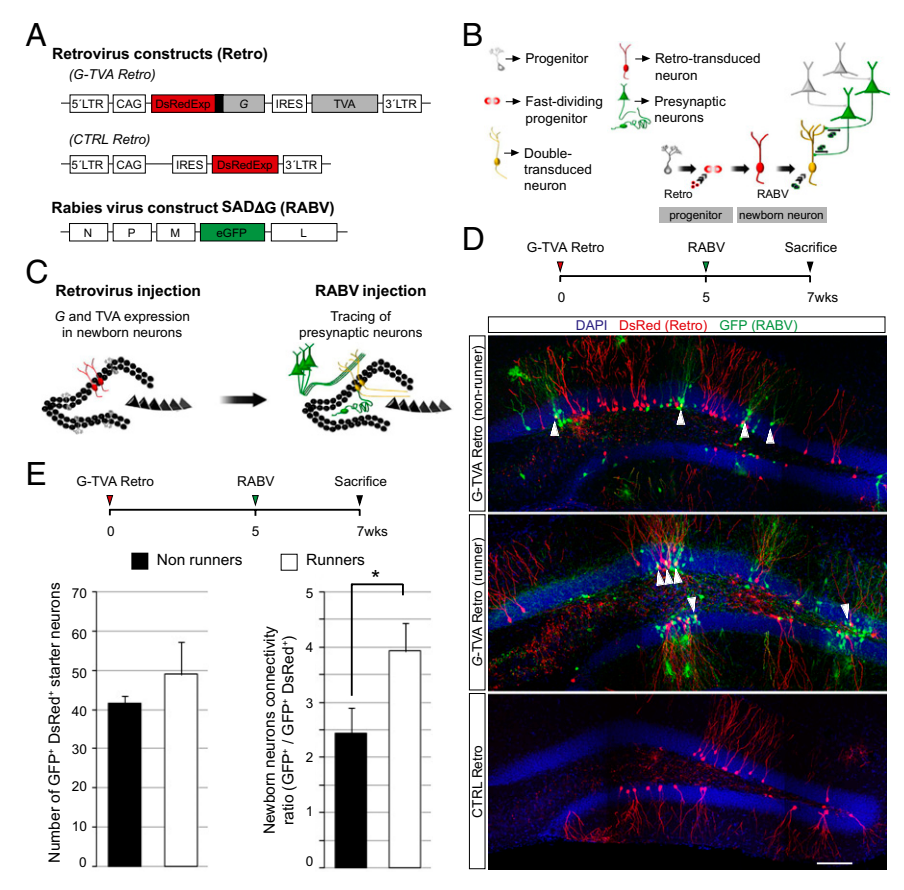


Fig. 1. RABV-mediated tracing of synapses onto adult-generated neurons in the DG. (A) Retroviral and RABV constructs. (B) Scheme of sequential virus delivery. (C) Implementation of the method in the DG of the hippocampus. Proliferating neural progenitors in the adult SGZ are transduced with the retrovirus, thus rendering them infectable by the RABV and their neuronal progeny capable of transsynaptic RABV transfer, followed by a second injection of RABV. Once synaptogenesis has taken place, RABV spreads from the primary infected neurons to their presynaptic partners. (D) Injection scheme used in the DG. Representative examples demonstrating the specificity of the system. Reconstructed confocal images from multiple fields depict cells labeled after injecting G and TVA encoding retrovirus in runner and nonrunner mice or control DsRed-only retrovirus, followed by RABV injection. White arrowheads: double transduced newborn neurons. (Scale bar, 50 μm.) (E) Absolute number of double-transduced starter neurons per mouse and ratio of RABV-transduced neurons in running mice compared with nonrunners (n = at least three mice per condition; *P < 0.05).

in animals subjected to voluntary wheel running, as reported previously (19), the number of primary RABV-infected starter cells was only moderately changed. Nonetheless, we observed a significant increase in the transsynaptic spread of RABV in running mice compared with nonrunners (Fig. 1 D and E). Thus, we focused our analyses on the presynaptic connectivity of adult-generated DG granule neurons of running mice. Importantly, upon RABV injection without prior retroviral transduction or following transduction with a control retrovirus encoding *DsRedExpress* only, no GFP⁺ neurons were observed in the DG, indicating that RABV infection was strictly dependent on *TVA* expression (Fig. 1D).

One concern is that already small amounts of TVA could suffice to render cells susceptible to RABV infection (21). Although retroviral vectors can only stably integrate into the genome of dividing cells, a nonintegrating viral infection can still result in transgene expression, a phenomenon called pseudotransduction (22), which may also allow nonproliferating cells to be susceptible to primary RABV infection. To test this possibility, we injected a TVA-only expressing retrovirus into the DG followed by RABV injection (Fig. S2 A and B). We observed double-transduced newborn granule neurons and a small proportion of GFP-only positive cells, even when RABV was injected 5 wk postretrovirus injection (Fig. S2 C-E). Notably, these GFP-only positive cells were restricted exclusively to the immediate vicinity of the injection site (Fig. S2C) and we never observed neurons labeled further away without retroviral delivery of G (n = 10 animals analyzed). Moreover, the proportion of GFP-only positive neurons under these experimental conditions was much lower in comparison with that obtained when a retrovirus encoding TVA and G was used (Fig. S2 D and E). These data suggest that a small proportion of mature neurons may indeed be pseudotransduced, causing them to express low but sufficient quantities of TVA, rendering them susceptible to RABV infection but unable to transfer RABV because of insufficient levels of G expression.

To eliminate the confounding effects of pseudotransduction, we took advantage of a mouse line expressing the TVA receptor under the control of the human glial fibrillary acidic protein (hGFAP) promoter (23, 24). In these mice, TVA is expressed in cells with an active hGFAP promoter, which also includes aNSCs residing in the SGZ of the DG that subsequently give rise to new granule neurons. We hypothesized that TVA protein expression may persist long enough to allow RABV infection in the progeny of aNSCs (Fig. 2 A and B), as previously reported (25). Indeed, stereotactic injection of RABV without retrovirus encoding G into the DG of hGFAP-TVA mice resulted in transduction of radial glia-like and horizontally oriented GFAP⁺ cells in the SGZ (Fig. 2 C-F) and a small proportion of neurons expressing the immature neuronal marker doublecortin (Dcx) (Fig. 2 E and F). Importantly, no neurons other than granule neurons were labeled in this paradigm. In contrast, when a retrovirus encoding G was injected into the SGZ 5 d before RABV injection, a small number of GFPonly positive neurons were detected in the SGZ and hilus (Fig. 2G). Thus, the use of hGFAP-TVA mice provides an alternative approach to target adult-generated neurons for RABV infection.

Temporal Evolution of the Presynaptic Connectivity of Adult-Born DG Granule Neurons. After thus validating the specificity and defining the respective limitations of the different strategies to target TVA (in addition to G) to adult-generated neurons as the starter cell population, we next proceeded to examine the temporal evolution of their presynaptic connectivity. For the first 2 wk following birth of adult-born granule neurons, we used the hGFAP-TVA mice, but for later time points analyses were performed on C57BL/6 mice using retroviral delivery of TVA (Fig. 3 A and G).

At the earliest time points analyzed in hGFAP-TVA mice (10 d following retroviral birth dating), we observed exclusively local neurons, \sim 70% of which were situated within the SGZ and GCL and the remainder within the hilus (Fig. 3 B and C). These data are consistent with the notion that GABAergic interneurons are among the first to form synapses onto adult-generated granule

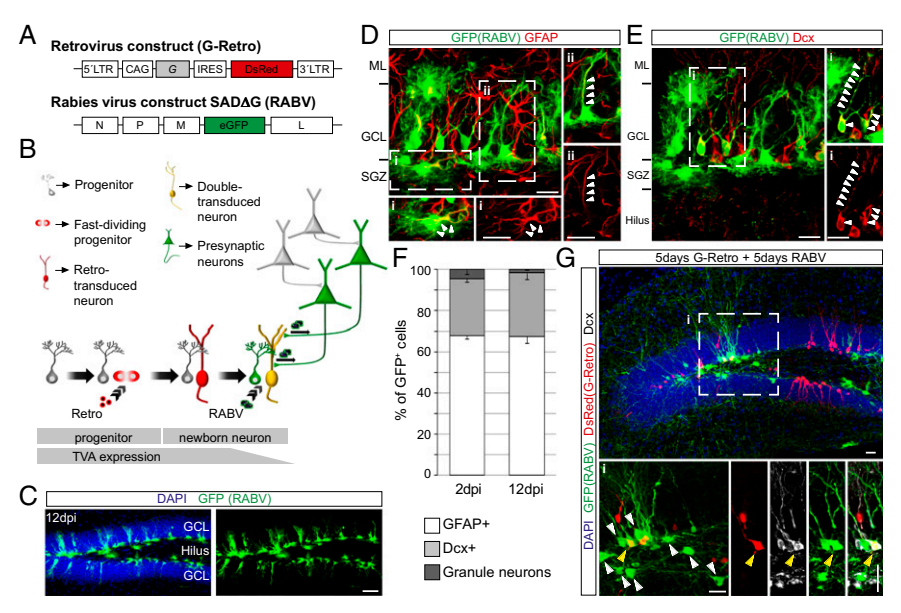


Fig. 2. Implementation of the RABV-mediated synaptic tracing in hGFAP-TVA mice. (*A*) Retroviral and RABV constructs. (*B*) Adaptation of the method to the hGFAP-TVA mouse line. Temporal profile of TVA expression is indicated by the lower bar. (*C*) Distribution of the cells targeted by EnvA-pseudotyped RABV in the DG of hGFAP-TVA mice 12 d postinjection (dpi). (Scale bar, 50 μm.) (*D*) Representative example of RABV-targeted cells in hGFAP-TVA mice comprising of GFAP+horizontal glia (*i*) and radial glia (*ii*). Enlargements show single and merged channels of the boxed areas, with arrowheads pointing to the colocalizing immunoreactive signal. (Scale bars, 20 μm.) (*E*) Example depicting Dcx+ newborn neurons targeted by RABV. Enlargement of the boxed area (*i*) shows the colocalization between GFP and Dcx (arrowheads). (Scale bars, 20 μm.) (*F*) Quantification of the identity of RABV-targeted cells in hGFAP-TVA mice at 2 and 12 dpi (n = 3 mice). (*G*) Example of RABV-traced presynaptic neurons at 10 d following injection of *G*-encoding retrovirus. Enlargements of the boxed area (*i*) show presynaptic neurons (white arrowheads) surrounding a double-transduced newborn neuron (yellow arrowhead). (Scale bars, 20 μm.)

Deshpande et al. PNAS Early Edition | 3 of 10

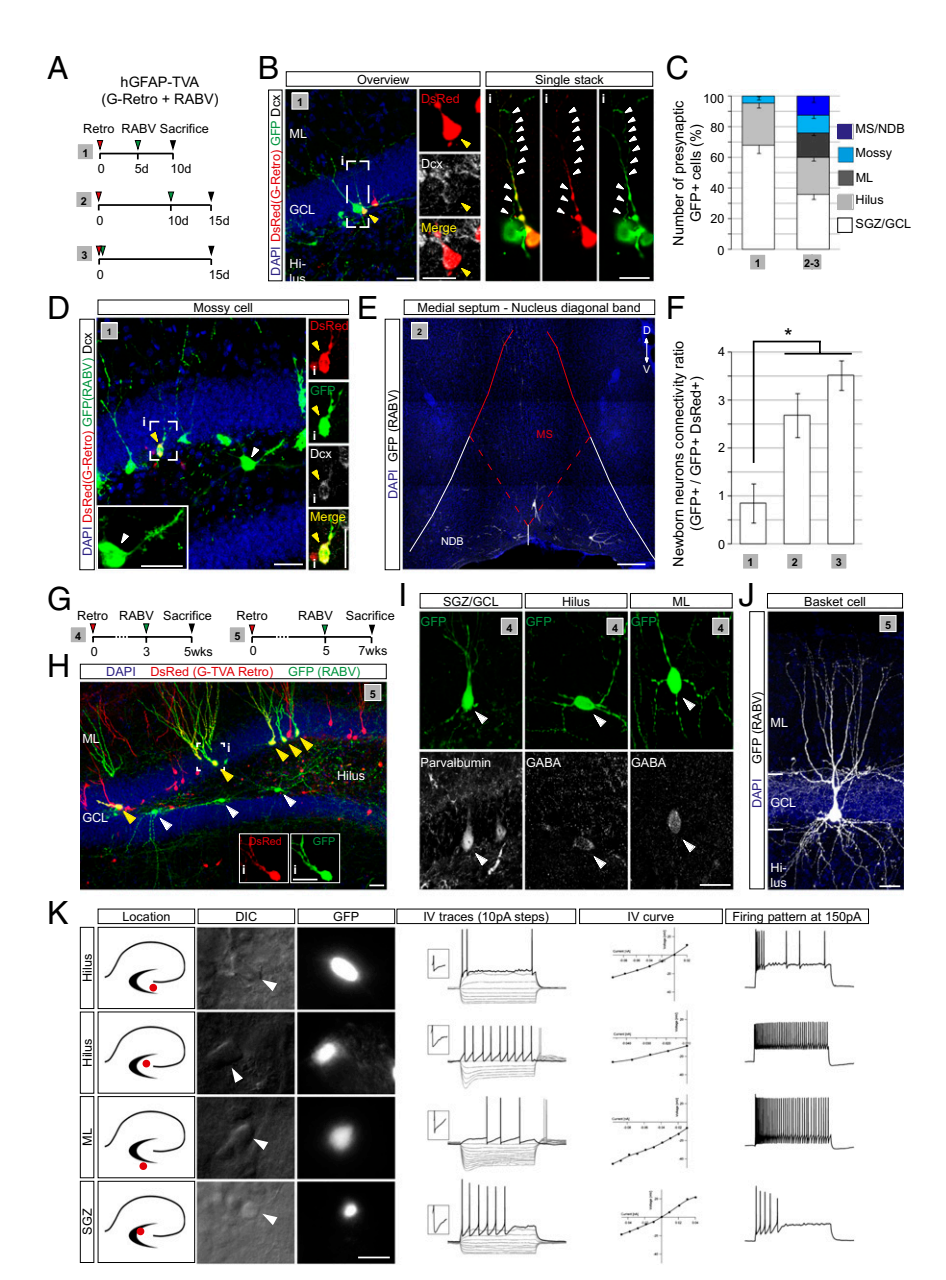


Fig. 3. Temporal development of the presynaptic connectome of newborn DG granule neurons. (A) Injection schemes (1-3) used in hGFAP-TVA mice. (B) Example of a presynaptic GFP-only positive neuron contacting a double-transduced newborn neuron (vellow arrowhead, enlarged in Insets). An individual stack of the boxed area (i) showing single and merged channels is depicted on the right. Arrowheads point to the axon of the presynaptic neuron. (Scale bars, 20 µm.) (C) Quantification of RABV-traced cells obtained following injection schemes (1-3) based on their morphology and location (n = 3-5). (D) Example of a RABV-traced mossy cell (white arrowhead, enlarged in the inset) located in the hilus of hGFAP-TVA mice following injection scheme 1. Enlargements of single and merged channels of a nearby double-transduced newborn neuron (yellow arrowhead, i) are shown on the right. (Scale bars, 30 µm.) (E) Example of RABV-traced neurons in the MS and NDB. (Scale bar, 70 μm.) (F) Ratio of RABV-traced neurons versus double-transduced newborn neurons following injection paradigms 1-3. (n = 3-5 mice per experimental condition; *P < 0.05). (G) Injection schemes (4 and 5) used in C57BL/6 mice. (H) Example of presynaptic tracing, 7 wk after retrovirus injection; double-transduced adult-generated granule neurons (yellow arrowheads) and putative presynaptic neurons (white arrowheads) are indicated. (Insets) Single channel images of the boxed cell. (Scale bars, 30 µM.) (/) Phenotypic characterization of RABVtraced local interneurons in the DG. (J) Example of a reconstructed RABV-traced basket cell profusely innervating the GCL. (Scale bars, 20 µm) (K) Visual and electrophysiological identification of presynaptic neurons in the DG and subiculum. GFP-only positive neurons (RABV-traced) were classified based on the location of their cell body (see micrographs) and the voltage responses following current injections. Several examples of presynaptic neurons differing in their IV traces and firing pattern are shown. (Scale bar, 20 µm.)

neurons (7, 26). Interestingly, this distribution of RABV-traced neurons changed within the following 5 d with the appearance of neurons in the molecular layer (ML) and the first long-range projection neurons residing in the medial septum (MS) and the nucleus of the diagonal band of Broca (NDB) (Fig. 3 C, E, and F). Additionally, among the GFP-labeled cells in the hilus already from the second week on, we also observed mossy cells, the local excitatory input to granule neurons in the DG (27). These cells were readily distinguishable by the characteristic thorny excrescences on their somata and proximal dendrites (Fig. 3 C and D). The same populations of local interneurons and mossy cells could also be traced at later time points in C57BL/6 mice (using retroviral TVA delivery). On the basis of their location within the DG and their morphology, neurochemical properties (Fig. 3 I and J) and electrophysiological properties (Fig. 3K), the majority of the neurons can be classified as local GABAergic interneurons (28), including parvalbumin-positive basket cells (Fig. 3*I*), somatostatin-positive hilar perforant path (HIPP) cells, hilar commissural-associational pathway (HICAP) cells, and interneurons residing in the ML as neurogliaform cells/Ivy cells,

or other molecular perforant path (MOPP) cells (28, 29) (Fig. S3). Intriguingly, the first long-range inputs onto newborn DG granule neurons arising from the MS/NDB were found to be cholinergic (Fig. 4 C and E). Finally, after 3 wk we could trace neurons located in the EC (Fig. 4 D and E) and these increased up to fivefold in number during the following 2 wk (Fig. 4 H and *I*). Surprisingly, we also observed GFP⁺ neurons located in the subiculum, a cortical structure adjacent to the hippocampus proper (Fig. 4 D and E), a projection that has not been described previously. Overall, our analysis revealed that besides the number of traced EC neurons, that of other presynaptic neurons also increased over time, with the exception of neurons in the MS/ NDB (Fig. 4 *G–I*). Fig. 4*J* summarizes the progressive emergence of presynaptic partners of adult-generated neurons in the DG starting from 5 d until 7 wk after their generation. Taken together, our data strongly support the notion that adult-born granule neurons receive first input from the local circuitry, followed by modulatory cholinergic (MS/NDB) and glutamatergic (mossy cell) synaptic input, before finally being incorporated into the classic hippocampal trisynaptic circuit upon innervation by the EC.

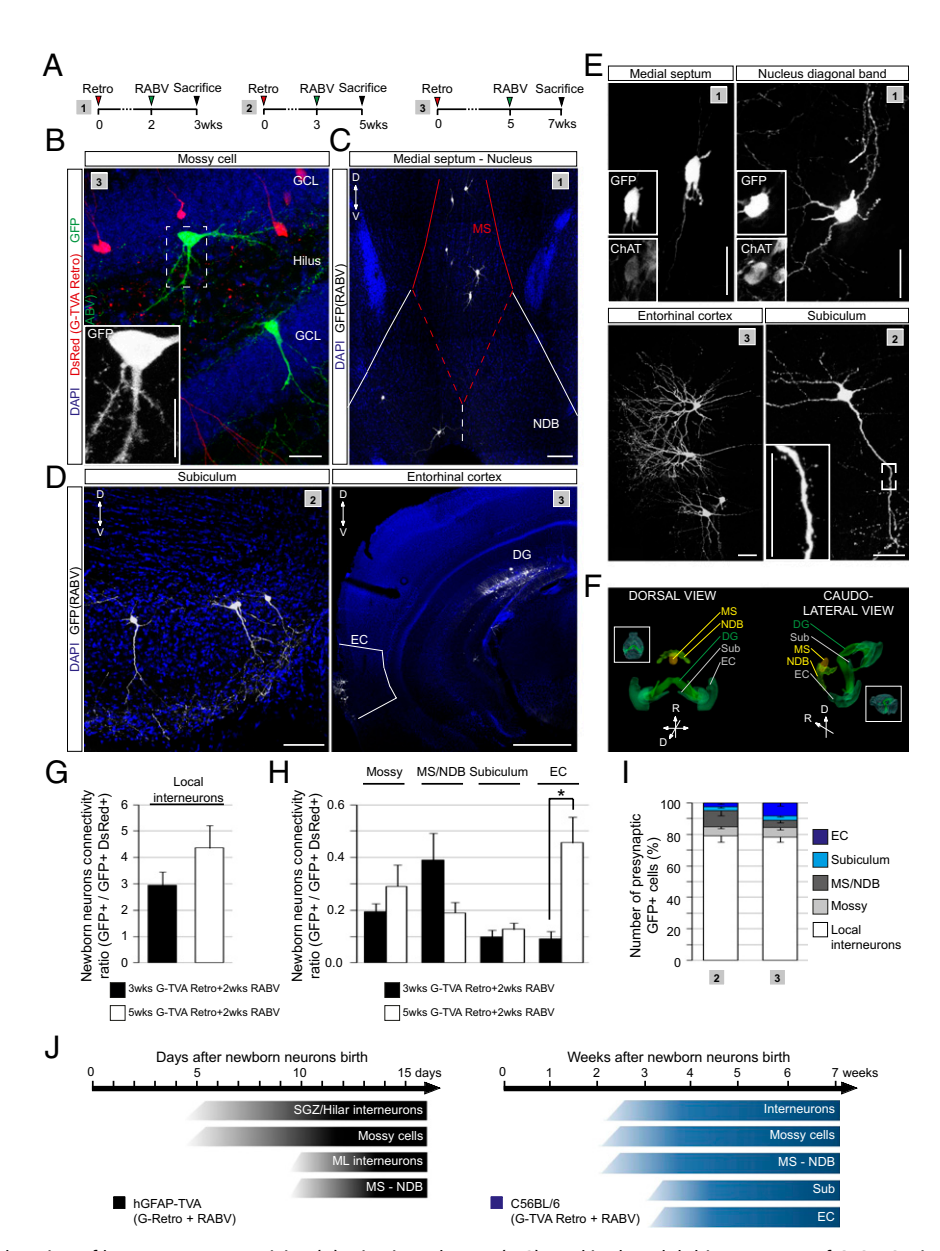


Fig. 4. RABV-mediated tracing of long-range connectivity. (*A*) Injection schemes (1–3) used in the adult hippocampus of C56BL6 mice. (*B*) Overview depicting the anatomical location of RABV-traced mossy cell (*Inset* shows enlarged image). (Scale bar, 20 μm.) (*C*) RABV-traced neurons in the MS and NDB. (Scale bar, 50 μm.) (*D*) Examples of RABV-traced neurons in the subiculum and the EC. [Scale bars, 50 μm (Subiculum) and 1 mm (EC).] (*E*) High magnification view of RABV-traced neurons in MS/NDB, EC, and subiculum. (*Inset*s) Colocalization of choline acetyltransferase (ChAT) with GFP in MS/NDB and the presence of spines on neurons in the subiculum. (Scale bars, 20 μm.) (*F*) Three-dimensional reconstruction of the anatomical locations of RABV-traced long-distance projection neurons; (*Inset*s) An entire brain view of the reconstructed anatomical regions. (*G*) Ratio of RABV-traced local interneurons versus double-transduced neurons following injection paradigms 2–3. (n = 4-6 mice per experimental condition; *P < 0.05). (*I*) Quantification of the identity of RABV-traced neurons obtained following injection paradigms 2–3 (n = 4-6 mice). (*I*) Summary of the identity and location of RABV-labeled presynaptic neurons appearing during the course of maturation of adult-born DG neurons in hGFAP-TVA and C57BL/6 mice.

Temporal and Spatial Evolution of the Presynaptic Connectivity of Adult-Born Olfactory Interneurons. Next we assessed whether the approach of retrovirus-based targeting of adult-generated neurons and transcomplementation with G for transsynaptic spread of RABV can also be adapted to the olfactory system comprised of the adult SEZ, the RMS, and the OB. We used two injection paradigms: In the first paradigm, the G- and TVA-encoding retrovirus was injected into the SEZ followed 4 d later by RABV injection into the RMS, to target retrovirus-transduced neuroblasts *en passant* while migrating toward the OB (Fig. 5A). In the second paradigm, RABV was delivered directly to the OB 28 or 56 d after retrovirus transduction, aiming at RABV infection of adult-generated neurons

following their integration in the OB (Fig. 5A). In both paradigms pseudotransduction is not of concern because of the large distance between the sites for retrovirus and RABV injection.

By 11 d following retroviral birth dating, the majority of the newborn neurons were already found in the OB (Figs. 5 *B* and *C* and 6*B*). RABV tracing resulted in the appearance of double-transduced granule cells in the GCL (Fig. 5 *A-C*). At that stage few RABV-traced presynaptic neurons were detected and they appeared strictly confined to the GCL. The number of local RABV-traced interneurons increased dramatically during the course of the next 7 d, being comprised of Blanes cells (within the GCL) and other short-axon cells (all layers of the OB), as

Deshpande et al. PNAS Early Edition | 5 of 10

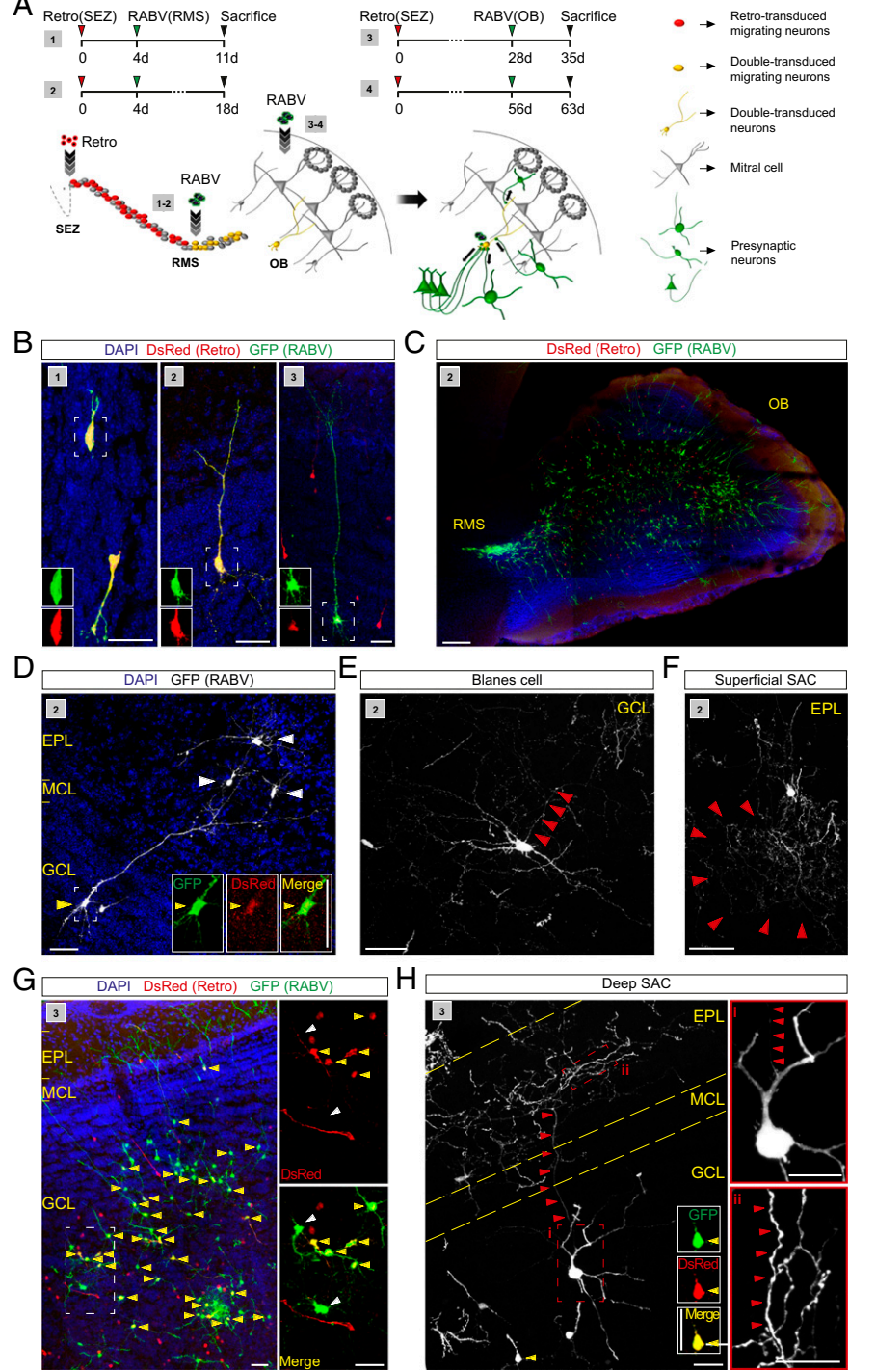


Fig. 5. RABV-mediated tracing of local presynaptic partners of adult-generated neurons in the OB. (A) Scheme of sequential virus delivery in two different injection paradigms (1 and 2). Injection of retrovirus into the SEZ, followed by RABV infection of migrating neuroblasts in the RMS (3 and 4). Injection of retrovirus into the SEZ, followed by RABV infection in the OB. (B) Double-transduced newborn granule cells at different stages of maturation obtained following injection schemes 1, 2, and 3. (Scale bar, 30 µm.) (C) Overview of RABV-labeled neurons in the OB following injection scheme 2. (Scale bar, 200 µm.) (D) Example of a double-transduced granule cell and RABV-traced superficial short axon cells (SACs) following RABV injection in the RMS. (Insets) Enlarged images of single and merged channels. (Scale bars, 50 um.) (E) Example of a RABVtraced Blanes cell in the GCL. Arrowheads point to the emerging axon. (Scale bar, 50 μm.) (F) Example of a RABV-traced superficial SAC in the EPL. (Scale bar, 50 µm.) (G) Overview of double-transduced (vellow arrowheads) and RABV-traced local neurons following RABV injection into the OB. A 3x digital zoom of the boxed area shows double-transduced and RABV-only transduced neurons (white arrowheads). (Scale bars, 50 μm.) (H) RABV-traced deep SAC following RABV injection in the OB. Note the doubletransduced cell (yellow arrowhead; Insets show single and merged channels); red arrowheads point to the ascending axon of the SAC. Boxed area (i) shows the cell body, with the emerging axon indicated by the arrowheads; area (ii) shows part of the axonal arborisation in the EPL. (Scale bars, 20 μm.)

assessed by morphology and location (30) (Fig. 5 D–F). From this stage and thereafter the number of local presynaptic neurons only increased slightly (Figs. 5 G and H, and G).

At 18 d following retroviral birth dating, the first RABV-traced neurons could be observed outside of the OB, namely within the anterior olfactory nucleus (AON) and the piriform cortex (Fig. 6 *A–F*), which are known to innervate granule cells via axodendritic synapses (31), and their number increased markedly in both areas up to 9 wk following retroviral birth dating (Fig. 6*J*). Conspicuously, RABV-traced neurons in the piriform cortex comprised different types of neurons, including superficial (Fig. 6*E*) and deep pyra-

midal cells (Fig. 6F) and, surprisingly, also some spineless neurons in layer III that may be the so-called smooth multipolar cells, believed to be GABAergic (Fig. 6G). These results show that, soon after their arrival in the OB, newborn neurons become targets for corticofugal control by the olfactory cortex (Fig. 6J and K).

To our surprise, we did not observe RABV-labeled mitral cells even after extended periods following RABV injection. As discussed below, the lack of RABV-tracing of mitral cells may be because of the particular type of reciprocal synapse between the OB principal neurons and OB granule or periglomerular cells, indicating an important limitation of the RABV-based tracing method.

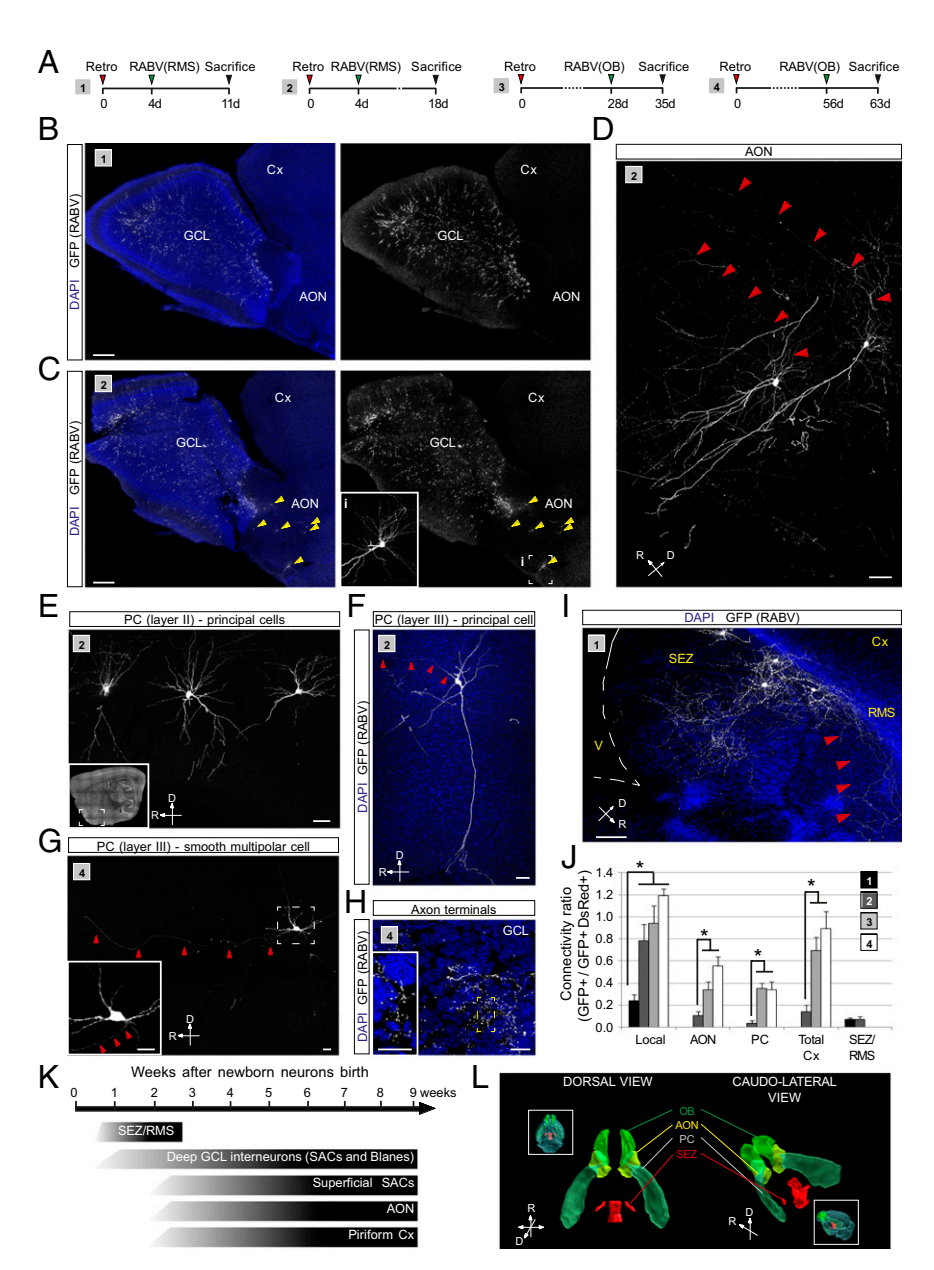


Fig. 6. RABV-mediated tracing of long distance projections of adult-generated neurons in the OB. (A) Injection schemes (1–4) used in adult C57BL/6 mice. (B and C) Overview of RABV-labeled neurons in the OB following injection scheme 1 (B) and 2 (C). Inset in C shows an enlargement of the boxed area (i) in the AON. (Scale bar, 200 μ m.) (D) Examples of RABV-traced neurons in the AON. Red arrowheads point to the emerging axons. (Scale bar, 30 μ m.) (E) RABV-traced long-distance projecting neurons located in layer II of the piriform cortex (PC) revealed following injection scheme 2; Inset shows the anatomical position of the neurons. (Scale bar, 20 μ m.) (F) RABV-traced deep pyramidal neurons located in layer III of the PC. (Scale bar, 20 μ m.) (G) RABV-traced smooth multipolar cell located in layer III of the PC. (Inset) Enlarged image of the boxed area. Red arrowheads point to the axon directed toward the OB. (Scale bars, 20 μ m.) (H) Axonal terminals of long-range projection neurons. Inset shows the numerous axonal boutons in the GCL. (Scale bars, 50 μ m.) (f) RABV-traced neurons in the observable of projection paradigms 1 and 2. Red arrowheads point to the axon of GFP-labeled neurons directed toward the RMS. (Scale bar, 50 μ m.) (f) Ratio of presynaptic neurons in different locations versus double-transduced neurons in the OB. (n = 3-4 mice per experimental condition; *P < 0.05). (K) Summary of the identity and location of RABV-labeled presynaptic neurons appearing during the course of maturation of adult-born granule cells in the OB. (L) Three-dimensional reconstruction of the anatomical locations of RABV-traced neurons.

Even more surprisingly, at the earliest stages analyzed, we observed RABV-traced neurons in close proximity of the SEZ and the RMS, revealing a dense axonal arborization within these two areas (Fig. 6I); these were labeled only upon RABV injection into the RMS. This finding suggests that migratory neuroblasts are transiently contacted by some mature neurons located in immediate vicinity of the SEZ/RMS. Thus, like in the DG, newborn neurons in the olfactory system first receive input from local GABAergic neurons before being innervated by long-range projection neurons located in the cortex (Fig. 6I). However, the

appearance of this cortical input occurs earlier when compared with the DG. Taking these data together—although with some notable limitations—RABV-tracing allows for unveiling the temporal evolution of the presynaptic connectivity of adult-generated neurons both in the hippocampus and olfactory bulb.

Discussion

We dissected the temporal evolution of the presynaptic connectome of adult-generated neurons in the two neurogenic zones of the forebrain, the DG and OB. To unravel the first-order

Deshpande et al. PNAS Early Edition | 7 of 10

presynaptic partners of these neurons, we made use of a versatile retrovirus-based technique for selectively targeting adult-generated neurons for primary RABV infection and subsequent retrograde RABV transfer. Studying the presynaptic connectivity of newly generated neurons at different stages following their birth revealed increasingly diverse populations of presynaptic partners, suggestive of their stepwise incorporation into functional neural circuits.

Consistent with previous electrophysiological studies (26, 32), newborn neurons in the adult DG become first innervated by interneurons in the SGZ and the hilus, and presynaptic connections from interneurons residing in the ML arrive slightly later, perhaps reflecting the maturation of the dendritic tree within the ML. Interestingly, newborn neurons receive input from hilar mossy cells very early on, thus being the first source of glutamatergic input to newborn granule neurons. Intriguingly, even before innervation by the EC, newborn neurons become innervated by modulatory cholinergic neurons in the MS/NDB. The rather late, but then very steeply increasing, innervation by the EC starting at 3 wk completes the integration of adult-generated neurons into the classic hippocampal circuitry. Moreover, we also observed a noncanonical innervation by the subiculum. As our analyses of the temporal evolution of presynaptic connectivity were confined to running mice, it cannot be excluded that such a pattern reflects the increase in hippocampal network activity as a result of physical activity. In fact, running mice exhibited an increase in presynaptic connectivity compared with sedentary mice, consistent with previous findings (20), suggesting that physical activity can alter the time course of integration.

On the other hand, newborn neurons in the OB become first innervated by a wide spectrum of local interneurons residing in the GCL (deep short-axon and Blanes cells), followed by interneurons (superficial short-axon cells) in the external plexiform layer (EPL). Rather early on newborn neurons in the OB also receive presumably glutamatergic input from neurons in the AON and piriform cortex. This corticofugal innervation is likely to exert a modulatory influence on newborn neurons' activity. Unfortunately, RABV-based tracing of monosynaptic connections did not allow for revealing the onset of input provided by mitral cells, thus leaving open at what stage newborn neurons are recruited into the reciprocal communication with the OB's principal cells.

Nevertheless, our results suggest that, despite the considerable differences in their respective local environment and cellular phenotype, the stepwise incorporation of adult-generated neurons into preexisting brain circuits follows remarkably similar principles in both neurogenic regions.

In line with the important role of the transmitter GABA for the initial stages of differentiation and maturation of newborn granule neurons (26), we found that their earliest presynaptic partners comprise local interneurons located in the SGZ-GCL, (e.g., parvalbumin-positive basket cells) (26), and within the hilus (e.g., HIPP cells) (28), suggesting that within the temporal resolution of our method, the very early innervation is not restricted to one single type of DG interneuron. Interestingly, innervations by interneurons whose somata and axonal arborization are located in the ML (e.g., so-called MOPP cells) appear to lag behind, which may reflect the time required for differentiation of the granule neuron dendrite within the ML. Occasionally, we also observed RABV-traced neurons classified as Ivy/neurogliaform cells, characterized by their compact dendritic tree and dense axonal arborization (29). Somewhat surprisingly, we detected labeling of hilar mossy cells starting from 5 to 10 d after the generation of newborn neurons, suggesting that these experience their first glutamatergic synaptic input from this type of hilar neuron. In addition, a recent study has suggested that early-stage newborn granule neurons receive massive but transient glutamatergic input from mature granule neurons (15). Although we also could detect some RABV-traced mature granule neurons, in our study they represented a minority. Furthermore, it cannot be excluded that these were traced as a consequence of pseudotransduction (i.e., direct infection by RABV following minute expression of TVA without retroviral integration) (Fig. S2C). Unfortunately, this issue could not be adequately resolved by the use of hGFAP-TVA mice, as a very small proportion of mature granule neurons express sufficient TVA receptor for primary infection. Remarkably, the ratio of synaptic input appeared to triple from the first to the second week of newborn neurons' life, alongside the emergence of mossy cells and the first MS/NDB inputs. During this stage, granule neurons also experience a switch of their GABA_A-receptor reversal potential, which ultimately converts the initially excitatory (depolarizing) action of GABA into an inhibitory one (26). Intriguingly, cholinergic innervations of newborn neurons arising from basal forebrain regions of the MS/NDB are likely to participate, via nicotinic receptor activation, in this developmental switch (33).

The striking increase in the number of presynaptic inputs observed by the end of the second week, the majority of which are still GABAergic in nature (>70%), immediately precede the formation of spines onto dendrites (i.e., presumable formation of excitatory synapses) (34, 35) and the functional maturation of axonal terminals of young granule neurons (6), two morphological correlates of successful neuronal integration. Given that at this stage the switch in GABA_A-receptor reversal potential is believed to have already taken place, our data may therefore indicate that by the moment young granule neurons become active players of the hippocampal network, inhibitory GABAergic inputs greatly outnumber excitatory glutamatergic ones. Such ratio of inhibitory versus excitatory inputs at this stage of their functional incorporation, may reflect a developmental condition of maintaining the highly excitable new neurons (4) under strong inhibition, and could thereby contribute to the selection of the forming excitatory synapses.

During the course of their maturation, we observed that adultgenerated DG granule neurons receive input from the subiculum, an intrahippocampal connection previously not well characterized. Using an anterograde neuronal tracer it was previously demonstrated that fibers originating in the presubiculum and parasubiculum of the subicular complex send a minor projection to the ML of the DG (36). The subiculum has been implicated in spatial navigation, memory processing, and stress response (37), functions in which newborn neurons play an important role (1, 2, 38, 39). As with the connections from the subiculum and well in agreement with previous morphological and electrophysiological studies (35, 40), labeling of neurons in the EC was observed only at later time points, with 3 wk after neurogenesis being the terminus post quem for a steep increase in synapse formation, very similar to the dramatic increase in the number of traced EC neurons observed by Vivar et al. (15). Such step-wise development of innervation may ensure that the functional incorporation of newborn DG granule neurons into the classic hippocampal trisynaptic circuit takes place only when they have reached functional maturity on the cellular level and have been already incorporated into the local circuit.

While in the DG only one type of neuron is generated, in the OB newborn neurons comprise a plethora of different types of interneurons located in different portions of the GCL and glomerular layer. This fact complicates assigning a specific population of presynaptic neurons to its postsynaptic newborn neuron population. In this study we either applied the RABV to the RMS, which would target newborn granule and periglomerular cells at the same time, or directly to the OB, where RABV infection depends primarily on the injection depth, in this case adjusted for the GCL. Given that most of the double-infected cells were granule cells, which is in agreement with the fact that the rate of granule cell generation is higher than that of periglomerular cells (41), it is probably safe to assume that the majority of presynaptic neuron populations identified here indeed form synapses onto

granule cells. To achieve a greater degree of specificity, approaches using cell type specific promoters may be required.

As in the DG, both local and long-range connections onto adult-generated neurons in the OB could be revealed; however, the method seems not to cover the full spectrum of presynaptic neurons, as indicated by the conspicuous absence of labeling of mitral or tufted cells using either of the two RABV injection paradigms employed in this study. A previous report using electroporation of TVA and G into early postnatal progenitors in the SEZ and subsequent RABV transduction in the OB resulted in the labeling of mitral cells (42). A potential explanation for this discrepancy may be a much slower maturation of synapses between mitral cells and adult-generated neurons, which in fact have been suggested to be preceded by centrifugal projections (31). Consistent with this finding, we observed labeled neurons in the olfactory cortex (AON and piriform cortex), known to form axo-dendritic synapses onto the basolateral dendrites of granule cells, already by the second week after retroviral birth-dating. Perhaps more importantly, lack of mitral and tufted cell labeling may be a direct consequence of the type of synapse rather than merely a result of the pace of synapse maturation. Although mitral cell axon collaterals form some axo-dendritic synapses onto OB granule cells (41), a majority of the synapses between these are reciprocal dendro-dendritic synapses. Whether mitral cell dendrites possess the machinery for efficient retrograde transport of RABV and whether this type of synapse is thus permissive for virus-transfer is currently unknown. Furthermore, whether and when mitral and tufted cells establish axo-dendritic synapses onto adult-generated neurons has not been revealed. In contrast to the absence of labeled mitral cells, other local presynaptic partners of newborn neurons were observed. Consistently labeled among these were the inhibitory deep and superficial short-axon cells, including Blanes cells, which display profuse axonal arborizations within the OB and are known to modulate granule cell activity through GABA (30, 43). Given that newborn neurons in the OB receive synaptic input before they show output activity, it can be speculated that short-axon cells may contribute to the proper functional integration of adult-born granule cells. Intriguingly, we also observed a transitory labeling of neurons located in or adjacent to the SEZ, which showed profuse axonal arborization covering the SEZ itself and the initial part of the RMS. Curiously, these neurons were detectable exclusively following RABV injection in the RMS and only during the first 2 wk after the birth of adult-born neurons. Because at this stage some of the starter population of cells was still found along the RMS or entering the OB, it is tempting to speculate that these presynaptic neurons form transient synapses with migrating newborn neurons, possibly supplying neurotransmitters during, and thereby affecting their journey to the OB (44, 45).

Retrovirus-based targeting of newborn neurons for RABV infection described herein can be used to map neuronal circuits remodeled by new neurons endogenously generated in the adult neurogenic areas (present study and ref. 15), as well as to study the incorporation of new neurons following transplantation (46) or even local reprogramming (47). Synaptic inputs are widely believed to play a key role in shaping the maturation and functional integration process of newly generated neurons (48), which are characterized by enhanced excitability and plasticity (49), allowing for their preferential recruitment into functional networks (50). Finally, this RABV-based approach is potentially suitable for the manipulation of those connections selectively impinging onto adult-generated neurons, thus permitting us to dissect the contribution of specific populations of presynaptic partners to the proposed unique role of young neurons in information processing.

Materials and Methods

Retrovirus Vector Construction. The retroviral construct used in this study was derived from a Moloney Murine Leukemia Virus-based retroviral vector in which

gene expression is driven by the chicken β -actin (CAG) promoter (40). The control retrovirus was constructed by subcloning DsRedExpress2 from pIRES2DsRedExpress2 (Clontech) into the CAG retroviral vector using BamHI and Notl restriction enzymes. For RABV-mediated transsynaptic tracing, a retroviral vector encoding the transgenes: the chicken TVA receptor, the RABV glycoprotein (G) from the CVS-11 strain of rabies virus, and a DsRedExpress2 reporter was constructed. DsRedExpress2 was excised from the plasmid pIRES2DsedExpress2 (Clontech) and replaced with the PCR-amplified cDNA for TVA800 (GPI-anchored form of TVA) to generate pIRES2-TVA using BstXI and NotI restriction enzymes. Primers were designed for the combined amplification of the 2A sequence, encoding the self-cleaving 2A peptide from the virus Thosea asigna and the cDNA for RABV G (2A-G) with Sall and Smal linkers. The 2A-G amplicon was cloned into pIRES2-TVA with these restriction enzymes. DsRedExpress2 without a translational stop codon was amplified by PCR from pIR-ES2DsRedExpress2 and cloned in-frame into p2A-G-IRES2-TVA using EcoRI and Sall. The entire DsRedExpress2-2A-G-IRES2-TVA cassette was subcloned using Sfil/NotI into the CAG retroviral vector (40) through the shuttle vector (pBKS-) to generate the polycistronic retroviral construct, CAG-DsRedExpress2-2A-G-IRES2-TVA. To generate CAG-G-IRES-DsRed, the RABV G was cloned into the CAG retroviral vector using Sfil/Pmel restriction enzymes through the shuttle vector pcDNA3.1. For the retroviral vector with TVA only (lacking G), the DsRedExpress2 reporter from pIRES2DsRedExpress2 was replaced with the PCR-amplified cDNA for TVA800 to generate pIRES2-TVA using BstXI and NotI restriction enzymes. The DsRedExpress2 from pIRES2DsedExpress2 was PCR amplified with EcoRI and Sall primers and cloned into pIRES2-TVA to generate pDsRedExp2-IRES2-TVA. The DsRedExp2-IRES2-TVA construct was then subcloned using Sfil/ Notl into the CAG retroviral vector through the shuttle vector (pBKS-) to generate the control retroviral construct, CAG-DsRedExpress2-IRES2-TVA.

Retrovirus Production. Retroviruses pseudotyped for the Vesicular Stomatitis Virus glycoprotein were produced as previously described (51, 52). Briefly, 75 μg of retroviral plasmid was used to transfect the helper-free HEK293gpg cell line using Lipofectamine 2000T. Virus was harvested at 2, 4, and 6 d posttransfection and concentrated by ultracentrifugation for in vivo injections and in vitro transduction. Titers used for experiments were typically in the range of 5–9 \times 10^7 .

Mice and Stereotactic Injections. *Mice.* Eight- to 10-wk-old C57BL/6 mice and transgenic mice expressing TVA under the human GFAP promoter (hGFAP-TVA) were used for injections. Animals were housed in groups of 2–4 and had unlimited access to running wheels from 7 to 10 d before retroviral injection. For nonrunners, animals were housed in cages without running wheels in groups of 2–4.

Virus injections. Mice were anesthetized using ketamine (100 mg/kg; CP-Pharma) and xylazine (5 mg/kg; Rompun; Bayer) and placed in a stereotactic apparatus. A small craniotomy was performed and \sim 0.5–1 μL of retrovirus or RABV was gradually injected at specific coordinates using a finely pulled capillary connected to a pulse generator and a vacuum pump. The skin incision was closed carefully after retroviral injection to minimize inflammation to facilitate the subsequent RABV injection. The following stereotactic coordinates were used relative to Bregma: for DG, caudal 2.0, lateral 1.6 and ventral 1.9–2.1; for SEZ, rostral 0.7, lateral 1.2 and ventral 1.6–2.0; for RMS, rostral 2.5, lateral 0.8 and ventral 3.2–3.0; for OB, rostral 4.5, lateral 0.8 and ventral 1.0–0.5. All animal procedures were performed in accordance to the Policies on the Use of Animals and Humans in Neuroscience Research, revised and approved by the Society of Neuroscience and the state of Bavaria under license no. 55.2-1-54-2531-144/07.

Histology and Immunostainings. Mice were deeply anesthetized using ketamine and xylazine and transcardially perfused with PBS for 5 min followed by $\sim\!150$ mL of 4% (wt/vol) paraformaldehyde for 25 min. The brains were extracted and postfixed for 1 h in 4% (wt/vol) paraformaldehyde at 4 °C sagittal or coronal sections at a thickness of 50–100 μm were cut at the vibratome. Sections were incubated overnight at 4 °C with primary antibodies diluted in blocking buffer [0.5% Triton-X-100 and 2% BSA (wt/vol) in PBS]. See SI Materials and Methods.

Electrophysiology. Preparation of brain slices. Five to 6 wk after retrovirus injection, C57BL/6 mice were deeply anesthetized with isoflurane, decapitated, and the brain was quickly removed into a chilled artificial cerebrospinal fluid (ASCF). Sagittal brain slices containing the hippocampus (300-µm thick) were prepared by using a vibratome (Microm HM650V; Microm International) and maintained at 28 °C for 1 h after cutting, followed by additional 1 h at room temperature. For recordings, slices were transferred into a recording chamber mounted on an upright microscope (Axioskop F5; Zeiss) equipped with a differential interference contrast optical device (DIC), infrared filter, and fluo-

Deshpande et al. PNAS Early Edition | 9 of 10

rescence filter sets (Zeiss filter set 38, 495/525 nm; Zeiss filter set 20HE, 560/ 607 nm). An infrared-sensitive CCD Hamamatsu camera (ORCA-R², Hamamatsu Photonics) was used for video-imaging during experiments.

Electrophysiological recordings and data analysis. Recordings were performed as previously described (53). Slices were constantly perfused at the rate of 1.5-2 mL/min with ACSF (125 mM NaCl, 3 mM KCl, 1.25 mM NaH₂PO₄, 2 mM CaCl₂, 2 mM MgCl₂, 25 mM NaHCO₃, and 25 mM p-glucose; pH 7.4) maintained at 28 °C and saturated with 95% O2 and 5%CO2. Whole-cell recordings were performed using microelectrodes (5-8 $M\Omega$) obtained from borosilicate glass capillaries (Clark Electromedical Instruments) filled with an internal solution having the following composition: 135 mM potassium gluconate, 4 mM KCl, 2 mM NaCl, 0.2 mM EGTA, 10 mM Hepes, 4 mM Mg-ATP, 0.5 mM Na-GTP, and 10 mM phosphocreatine (pH 7.3, osmolarity 290 mOsm). Current-clamp recordings (ELC-03XS amplifier; NPI) were filtered at 10 kHz, digitized at a rate of 2-5 kHz using an analog/ digital-converter (PCI-6024E; National Instruments) and acquired using the program CellWorks (NPI). Cells were selected for subsequent analysis depending on their fluorescence emission (eGFP+ or DsRed+) and location in the hippocampal formation. After recording, visual confirmation of the

- 1. Nakashiba T. et al. (2012) Young dentate granule cells mediate pattern separation. whereas old granule cells facilitate pattern completion. Cell 149(1):188-201.
- 2. Aimone JB, Deng W, Gage FH (2011) Resolving new memories: A critical look at the dentate gyrus, adult neurogenesis, and pattern separation. Neuron 70(4):589-596.
- 3. Alonso M, et al. (2012) Activation of adult-born neurons facilitates learning and memory. Nat Neurosci 15(6):897-904.
- 4. Marín-Burgin A, Mongiat LA, Pardi MB, Schinder AF (2012) Unique processing during a period of high excitation/inhibition balance in adult-born neurons. Science 335(6073):1238-1242.
- Bardy C, Alonso M, Bouthour W, Lledo PM (2010) How, when, and where new inhibitory neurons release neurotransmitters in the adult olfactory bulb. J Neurosci 30(50):17023-17034
- 6. Toni N, et al. (2008) Neurons born in the adult dentate gyrus form functional synapses with target cells. Nat Neurosci 11(8):901-907.
- 7. Esposito MS, et al. (2005) Neuronal differentiation in the adult hippocampus recapitulates embryonic development. J Neuroscience 25(44):10074-10086.
- 8. Laplagne DA, et al. (2006) Functional convergence of neurons generated in the developing and adult hippocampus. PLoS Biol 4(12):e409.
- Wickersham IR, et al. (2007) Monosynaptic restriction of transsynaptic tracing from single, genetically targeted neurons. Neuron 53(5):639-647.
- 10. Wickersham IR, Finke S, Conzelmann KK, Callaway EM (2007) Retrograde neuronal tracing with a deletion-mutant rabies virus. Nat Methods 4(1):47-49.
- 11. Marshel JH, Mori T, Nielsen KJ, Callaway EM (2010) Targeting single neuronal networks for gene expression and cell labeling in vivo. Neuron 67(4):562-574.
- 12. Miyamichi K, et al. (2011) Cortical representations of olfactory input by trans-synaptic tracing. Nature 472(7342):191-196.
- 13. Stepien AE, Tripodi M, Arber S (2010) Monosynaptic rabies virus reveals premotor network organization and synaptic specificity of cholinergic partition cells. Neuron 68(3):456-472.
- 14. Wall NR, Wickersham IR, Cetin A, De La Parra M, Callaway EM (2010) Monosynaptic circuit tracing in vivo through Cre-dependent targeting and complementation of modified rabies virus. Proc Natl Acad Sci USA 107(50):21848-21853.
- Vivar C, et al. (2012) Monosynaptic inputs to new neurons in the dentate gyrus. Nat Commun 3:1107.
- 16. Ming GL, Song H (2005) Adult neurogenesis in the mammalian central nervous system, Annu Rev Neurosci 28:223-250.
- Brill MS, et al. (2009) Adult generation of glutamatergic olfactory bulb interneurons. Nat Neurosci 12(12):1524-1533.
- 18. Lledo PM, Merkle FT, Alvarez-Buylla A (2008) Origin and function of olfactory bulb interneuron diversity. Trends Neurosci 31(8):392-400.
- 19. van Praag H. Kempermann G. Gage FH (1999) Running increases cell proliferation and neurogenesis in the adult mouse dentate gyrus. Nat Neurosci 2(3):266-270.
- 20. Piatti VC, et al. (2011) The timing for neuronal maturation in the adult hippocampus is modulated by local network activity. J Neurosci 31(21):7715-7728.
- Bates P, Young JA, Varmus HE (1993) A receptor for subgroup A Rous sarcoma virus is related to the low density lipoprotein receptor. Cell 74(6):1043-1051.
- 22. Haas DL, Case SS, Crooks GM, Kohn DB (2000) Critical factors influencing stable transduction of human CD34(+) cells with HIV-1-derived lentiviral vectors. Mol Ther 2(1):71-80.
- 23. Holland EC, Hively WP, DePinho RA, Varmus HE (1998) A constitutively active epidermal growth factor receptor cooperates with disruption of G1 cell-cycle arrest pathways to induce glioma-like lesions in mice. Genes Dev 12(23):3675-3685.
- 24. Holland EC, Varmus HE (1998) Basic fibroblast growth factor induces cell migration and proliferation after glia-specific gene transfer in mice. Proc Natl Acad Sci USA
- 25. Doetsch F, Caillé I, Lim DA, García-Verdugo JM, Alvarez-Buylla A (1999) Subventricular zone astrocytes are neural stem cells in the adult mammalian brain. Cell 97(6):703-716.
- 26. Ge S, et al. (2006) GABA regulates synaptic integration of newly generated neurons in the adult brain. Nature 439(7076):589-593.
- 27. Amaral DG, Scharfman HE, Lavenex P (2007) The dentate gyrus: Fundamental neuroanatomical organization (dentate gyrus for dummies). Prog Brain Res 163:3-22.

identity of the recorded cell was achieved by controlling the fluorescent signal in the pipette tip. Off-line data analysis was performed with Igor Pro-6 software (WaveMetrics).

ACKNOWLEDGMENTS. We thank Dr. Heiko Lickert (HelmholtzZentrum Munich) for kindly providing the 2A peptide sequence; Dr. Matthias Stanke (Institute for Cell Biology and Neuroscience Frankfurt) for the hGFAP-TVA mice; Dr. Bernd Sutor (Ludwig-Maximilians University Munich) for help with the electrophysiology; Dr. Veronica Egger for insightful suggestions; Nadin Hagendorf, Detlef Franzen, Gabi Jaeger, and Tatiana Simon-Ebert for excellent technical assistance; and J. A. Young and I. Wickersham for kindly providing the pCMMP-TVA800 plasmid and BHK-EnvARGCD and 293T-TVA800 cells. This work was supported by grants from the Bundesministerium für Bildung und Forschung "Integration of stem cell derived neurons," the Bavarian State Ministry of Sciences, Research and the Arts (to M.G. and B.B.); by the CRC 1080 from the Deutsche Forschungsgemeinschaft (to B.B.); by the German Excellence Initiative via the "Cluster of integrated protein Sciences" (to M.G. and A.D.); and by the SFB 870 from the Deutsche Forschungsgemeinschaft (to M.G. and K.-K.C.). M.B. is a recipient of a Ludwig-Maximilians University Research Fellowship.

- 28. Freund TF. Buzsáki G (1996) Interneurons of the hippocampus. Hippocampus 6(4): 347-470
- 29. Markwardt SJ, Wadiche JI, Overstreet-Wadiche LS (2009) Input-specific GABAergic signaling to newborn neurons in adult dentate gyrus. J Neurosci 29(48):15063-15072.
- 30. Pressler RT, Strowbridge BW (2006) Blanes cells mediate persistent feedforward inhibition onto granule cells in the olfactory bulb. Neuron 49(6):889-904.
- 31. Whitman MC, Greer CA (2007) Synaptic integration of adult-generated olfactory bulb granule cells: basal axodendritic centrifugal input precedes apical dendrodendritic local circuits. J Neurosci 27(37):9951-9961.
- 32. Markwardt S, Overstreet-Wadiche L (2008) GABAergic signalling to adult-generated neurons. J Physiol 586(16):3745-3749.
- 33. Campbell NR, Fernandes CC, Halff AW, Berg DK (2010) Endogenous signaling through alpha7-containing nicotinic receptors promotes maturation and integration of adultborn neurons in the hippocampus. J Neurosci 30(26):8734-8744.
- 34. Zhao C, Teng EM, Summers RG, Jr., Ming GL, Gage FH (2006) Distinct morphological stages of dentate granule neuron maturation in the adult mouse hippocampus. J Neuroscience 26(1):3-11.
- 35. Toni N, et al. (2007) Synapse formation on neurons born in the adult hippocampus. Nat Neurosci 10(6):727-734.
- 36. Köhler C (1985) Intrinsic projections of the retrohippocampal region in the rat brain. I. The subicular complex. J Comp Neurol 236(4):504-522.
- 37. O'Mara S (2005) The subiculum: What it does, what it might do, and what neuroanatomy has yet to tell us. J Anat 207(3):271-282.
- 38. Sahay A, et al. (2011) Increasing adult hippocampal neurogenesis is sufficient to improve pattern separation. Nature 472(7344):466-470.
- 39. Santarelli L. et al. (2003) Requirement of hippocampal neurogenesis for the behavioral effects of antidepressants. Science 301(5634):805-809.
- 40. van Praag H, et al. (2002) Functional neurogenesis in the adult hippocampus. Nature 415(6875):1030-1034.
- 41. Shepherd G (2003) Synaptic Organization of the Brain (Oxford Univ Press, New York) 5th Ed.
- 42. Arenkiel BR, et al. (2011) Activity-induced remodeling of olfactory bulb microcircuits revealed by monosynaptic tracing, PLoS ONE 6(12):e29423.
- 43. Eyre MD, Antal M, Nusser Z (2008) Distinct deep short-axon cell subtypes of the main olfactory bulb provide novel intrabulbar and extrabulbar GABAergic connections. J Neuroscience 28(33):8217-8229.
- 44. Carleton A, Petreanu LT, Lansford R, Alvarez-Buylla A, Lledo PM (2003) Becoming a new neuron in the adult olfactory bulb. Nat Neurosci 6(5):507-518.
- 45. Bolteus AJ, Bordey A (2004) GABA release and uptake regulate neuronal precursor migration in the postnatal subventricular zone. J Neuroscience 24(35):7623-7631.
- 46. Gaillard A, Jaber M (2011) Rewiring the brain with cell transplantation in Parkinson's disease. Trends Neurosci 34(3):124-133.
- 47. Rouaux C, Arlotta P (2010) Fezf2 directs the differentiation of corticofugal neurons from striatal progenitors in vivo. Nat Neurosci 13(11):1345-1347.
- 48. Bergami M, Berninger B (2012) A fight for survival: The challenges faced by a newborn neuron integrating in the adult hippocampus. Dev Neurobiol 72(7):1016-1031.
- 49. Mongiat LA, Schinder AF (2011) Adult neurogenesis and the plasticity of the dentate gyrus network. Eur J Neurosci 33(6):1055-1061
- 50. Kee N, Teixeira CM, Wang AH, Frankland PW (2007) Preferential incorporation of adult-generated granule cells into spatial memory networks in the dentate gyrus. Nat Neurosci 10(3):355-362.
- 51. Pear WS, Nolan GP, Scott ML, Baltimore D (1993) Production of high-titer helper-free retroviruses by transient transfection. Proc Natl Acad Sci USA 90(18):8392-8396.
- Yee JK, Friedmann T, Burns JC (1994) Generation of high-titer pseudotyped retroviral vectors with very broad host range. Methods Cell Biol 43(Pt A):99-112.
- 53. Zolles G, Wagner E, Lampert A, Sutor B (2009) Functional expression of nicotinic acetylcholine receptors in rat neocortical layer 5 pyramidal cells. Cereb Cortex 19(5): 1079-1091